



# CHORUS

This is the accepted manuscript made available via CHORUS. The article has been published as:

## Role of the spatial inhomogeneity on the laser-induced vacuum decay

Q. Z. Lv, S. Dong, Y. T. Li, Z. M. Sheng, Q. Su, and R. Grobe

Phys. Rev. A **97**, 022515 — Published 27 February 2018

DOI: [10.1103/PhysRevA.97.022515](https://doi.org/10.1103/PhysRevA.97.022515)

# Role of the spatial inhomogeneity on the laser-induced vacuum decay

Q.Z. Lv<sup>1,2,3</sup>, S. Dong<sup>3,4</sup>, Y.T. Li<sup>1</sup>, Z.M. Sheng<sup>4</sup>, Q. Su<sup>3</sup> and R. Grobe<sup>3</sup>

(1) Beijing National Laboratory for Condensed Matter Physics, Institute of Physics,  
Chinese Academy of Sciences, Beijing 100190, China

(2) Max Planck Institute for Nuclear Physics, Saupfercheckweg 1, 69117 Heidelberg, Germany

(3) Intense Laser Physics Theory Unit and Department of Physics  
Illinois State University, Normal, IL 61790-4560, USA

(4) School of Physics and Astronomy, Collaborative Innovation Center of IFSA,  
Shanghai Jiao Tong University, Shanghai 200240, China

This study suggests that the unavoidable spatial inhomogeneity of intense electromagnetic fields has a drastic effect on the electron-positron pair creation process from the vacuum. We use the example of the Breit-Wheeler process, where the collision of two gamma-ray photons is predicted to create electron-positron pairs, to show that the multi-photon pair creation process cannot be modeled by solutions to the Dirac equation under time-periodic fields that are spatially homogeneous. The neglect of the spatial inhomogeneity leads here to spurious energy spectra and misleading pair creation yields that can be incorrect by up to several orders in magnitude. This finding is surprising as there are many widely cited works where the laser is modeled by a spatially homogeneous alternating electric field.

Present high-power laser facilities have reached intensities  $I_0 \sim 10^{22}$  W/cm<sup>2</sup> and upcoming 10-PW facilities aim at  $I_0 \sim 10^{23}$  W/cm<sup>2</sup> [1]. Such technological achievements render lasers a feasible tool for probing the nonlinear properties of the quantum electrodynamical vacuum state at field strengths effectively of the order of  $E_{cr} = 1.3 \times 10^{16}$  V/cm [2]. In the presence of an external field  $E_{cr}$ , the vacuum becomes unstable and decays into particle-antiparticle pairs.

There are two intrinsically different mechanisms by which electron-positron pairs can be created from the vacuum. The first scheme [3] requires the field (which can be static) to be extremely strong and can be visualized in terms of a tunneling process between energy shifted Dirac states, while the second scheme [4] requires a very large laser frequency that can trigger the transition between the positive and negative energy states. Both regimes can be characterized by the ratio of the laser's frequency  $\omega$  and its electric field amplitude  $E_f$ , given by Keldysh's adiabaticity parameter [5]  $\gamma_K \equiv m\omega c/(qE_f)$ . Pair creation has been thoroughly investigated by approximating the laser as an alternating electric field that is homogeneous in space [6]. Similarly, the omission of the spatial dependence in  $\sin[\omega(t-x/c)]$ , leading to  $\sin(\omega t)$ , was also motivated by "focusing on the anti-nodal region" [7] of two counter-propagating linearly polarized beams, e.g., replacing  $\sin[\omega(t-x/c)] + \sin[\omega(t+x/c)] = 2 \sin(\omega t) \cos(\omega x/c)$  by  $2 \sin(\omega t)$ . From a theoretical point of view, this simplification is very advantageous, as the total canonical momentum of the system becomes conserved, which permits us to employ powerful theoretical techniques (quantum kinetic Vlasov equation, imaginary time or WKB methods, time-dependent perturbation theory, etc.) to study the pair-creation process. We are not aware of any study in which the validity of this simplification has been examined quantitatively.

However, there have been various studies that have included the inhomogeneity of these fields by using methods other than the quantum kinetic approach. These include, for instance, the worldline instanton technique [8], the Dirac-Heisenberg-Wigner formalism [9], nonperturbative techniques [10] and scalar and fermionic free field theories [11]. For example, the Dirac-Heisenberg-Wigner formalism [12,13] also allows us to investigate the production of electron-positron pairs from a transport/kinetic view point, but includes a full space-time dependence in the external laser fields. An independent numerical approach was developed recently by Aleksandrov, Plunien, and Shabaev [14]. They have considered the electron-positron pair creation induced by factorized fields in space and time. Complementing this work, our research here examines the Breit-Wheeler effect, even though our algorithm in principle can be

applied to arbitrary external field configurations.

It is the purpose of the present work to suggest that the omission of the laser's spatial inhomogeneity in the high-frequency regime ( $\gamma_K \gg 1$ ) changes the entire pair-creation process and therefore leads to unreliable predictions. For example, the energy spectra of the created particles are qualitatively incorrect and contain spurious unphysical peaks. Also, the pair creation rates can differ by several orders in magnitude from the true rates. Moreover, because of the significant quantitative differences between the spectra obtained for a spatially dependent laser beam and those generated by a homogeneous alternating field, the present results will also be useful for the design of upcoming intense laser facilities aiming at measuring these multi-photon processes [15-17].

We illustrate our findings for the Breit-Wheeler (BW) process, which describes the creation of a real electron-positron pair as the result of the collision of two highly energetic photons with a center of mass energy exceeding  $2mc^2 = 1.02$  MeV. This process is among the most fascinating textbook examples of quantum electrodynamics, as it provides the most direct way to convert electromagnetic energy into mass. It also requires us to give up the concept of linear superposition for the Maxwell equations and points to the nonlinear character of electromagnetism. While this process has not been verified experimentally yet, its generalized version such as the matter-assisted electron-positron creation (scattering of ultra-relativistic electron beams with laser beams [18], intense laser-plasma interactions [19] and laser-driven solid target scattering [20]) have been observed. Historically, the BW process has been modeled by the Dirac equation, in which the two colliding photons are approximated by two classical electromagnetic plane wave fields with frequency  $\omega$  each and wave number  $k = \omega/c$ .

Let us first briefly summarize our approach [21] based on computational quantum field theory. The interaction of the electromagnetic field with the electron-positron quantum field operator is described by the usual Dirac Hamiltonian  $H = c \boldsymbol{\alpha} [\mathbf{p} - q\mathbf{A}(\mathbf{r},t)/c] + mc^2 \beta$ , where  $\boldsymbol{\alpha} \equiv (\alpha_1, \alpha_2, \alpha_3)$  and  $\beta$  denote the set of the four  $4 \times 4$  Dirac matrices,  $m$  and  $q$  are the electron's mass and charge and  $c$  is the speed of light. If the electronic and positronic spins are aligned along the direction of the corresponding magnetic field  $\nabla \times \mathbf{A}(\mathbf{r},t)$ , they are conserved, which simplifies the computational analysis. The initial vacuum state is represented by the set of occupied eigenstates  $|d;p\rangle$  of the (field-free) Dirac operator  $H_0$  with negative energy that satisfy  $H_0|d;p\rangle = -[m^2 c^4 + c^2 p^2]^{1/2} |d;p\rangle$ . The corresponding positive-energy states with momentum  $p$  are denoted by  $|u;p\rangle$ . In computational quantum field theory the required space-time evolution of the electron-positron quantum field

operator can be obtained equivalently from the quantum mechanical evolution of the complete set of all states  $|d;p\rangle$  and the resulting matrix elements  $U_{pn}(t) \equiv \langle u;p|U(t)|d;p\rangle$ , where  $U(t)$  is the time-ordered evolution operator associated with  $H$ . These solutions of the space-time dependent Dirac equation with the vector potential  $\mathbf{A}(\mathbf{r},t)$  can be obtained on a space-time lattice using efficient fast-Fourier transformation based split-operator techniques. The number of created electron-positron pairs after the interaction of duration  $T$  is then obtained from all time-evolved Hilbert-space states as  $N(T) \equiv \sum_{pn} |U_{pn}(T)|^2$  and the energy distribution of the created electrons is given by  $\rho(E,T) \equiv \sum_n |U_{pn}(T)|^2$ . We note that this approach is different from [22], where the vacuum was approximated by a single negative-energy Gaussian wave packet at rest. This pioneering work pointed out that two counter-propagating beams can lead to Autler-Townes-split resonance peaks.

In general, external electromagnetic fields have a dual impact on the dynamics. They can lead to a reversible dressing as well as to permanent quantum transitions. It is well known that a monochromatic linearly polarized beam of photons with energy  $\hbar\omega$ , e.g., described by the potential  $\mathbf{A}(\mathbf{r},t) = A_0 \sin[\omega(t-x/c)] \mathbf{e}_y$ , solely dresses electronic eigenstates (Volkov states) and therefore cannot induce any irreversible transitions between different states once the field is turned off. In other words, a beam of identical photons cannot create any electron-positrons pairs, similar to the fact that a free electron cannot absorb a photon in the absence of any other forces. On the other hand, a "mathematical" vector potential  $\mathbf{A}(t) = A_0 \sin(\omega t) \mathbf{e}_y$  (where the spatial dependence was artificially removed) can trigger numerous irreversible transitions from the negative to the positive energy manifold, therefore it predicts (incorrectly) the creation of electron-positron pairs. In order to avoid any confusion, we remark that in a non-relativistic treatment (governed by the usual Schrödinger equation) the potential  $\mathbf{A}(t)$  does permit analytical Volkov-like solutions. This means that here the potential  $\mathbf{A}(t)$  solely dresses the state and therefore cannot induce any quantum transitions, which is in direct contrast to its effect within the relativistic framework of the Dirac equation that we will examine below.

Before the quantitative results are presented, let us discuss some important qualitative differences between the two dynamics induced by the fields  $\mathbf{A}(t) = A_0 \sin(\omega t) \mathbf{e}_y$  and  $\mathbf{A}(\mathbf{r},t) = A_0 \sin(\omega t) \cos(kx) \mathbf{e}_y$  with  $\hbar\omega > 2mc^2$ . In the left panel of Figure 1 we sketch the possible transitions from the negative to the positive energy manifold triggered by the alternating field  $\mathbf{A}(t)$ . Due to the assumption of spatial homogeneity, there are two unphysical transitions resulting in peaks in the energy spectrum of the created electrons. The lowest energetic peak occurs at  $E = \hbar\omega/2$  and is

associated with an unphysical "one-photon" coupling from the initially populated negative energy state  $|d;p\rangle$  with energy  $-\hbar\omega/2$  ( $< -mc^2$ ) directly to the positive energy state with energy  $\hbar\omega/2$ .

Similarly, a second unphysical peak at  $3\hbar\omega/2$  is associated with the additional transition within the positive energy manifold.

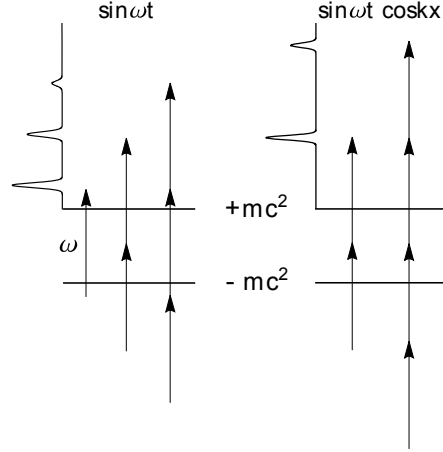


Figure 1 Left panel: The (mathematically) predicted transitions from the Dirac sea to positive energy states if the laser field is modelled by the spatially homogeneous potential  $\mathbf{A}(t) = A_0 \sin(\omega t) \mathbf{e}_y$  with frequency  $\omega = 3mc^2/\hbar$ . Right panel: For comparison, the true transitions associated with two counter-propagating laser beams given by the potential  $\mathbf{A}(\mathbf{r},t) = A_0 \sin(\omega t) \cos(kx) \mathbf{e}_y$ .

For comparison, on the right panel we have sketched the (physically permitted) transitions associated with two counter-propagating laser beams of the same frequency, i.e,  $\mathbf{A}(\mathbf{r},t) = A_0 \sin(\omega t) \cos(x\omega/c) \mathbf{e}_y$ . Here the lowest peak energies of created electrons occur at  $E = \hbar\omega$  and  $2\hbar\omega$ , corresponding to the permitted Breit-Wheeler processes  $2\gamma \rightarrow e^- + e^+$  and  $4\gamma \rightarrow e^- + e^+$ . We see that there are no peaks at all at energies  $E = \hbar\omega/2$  and  $3\hbar\omega/2$ . While the peak locations  $E = \hbar\omega$  and  $2\hbar\omega$  were predicted correctly by the field  $\mathbf{A}(t)$ , we show below that  $\mathbf{A}(t)$  fails completely to predict the associated amplitudes.

In Figure 2 we show the non-trivial growth of the number of created electron-positron pairs  $N(t)$  as two counter-propagating laser pulses with frequency  $\omega = 1.25mc^2/\hbar$  collide with each other. While the detailed properties of the created particle pairs depend on the specific features of the laser fields, in order to capture the qualitative features of two counter-propagating plane wave laser fields with same frequency, we have modeled the laser by  $\mathbf{A}(\mathbf{r},t) = A_0 [F_R(x,t) \sin(\omega t - kx) + F_L(x,t) \sin(\omega t + kx)] \mathbf{e}_y$ , with  $F_R(x,t) = (\text{Tanh}[(x-x_R+d/2-ct)/w] - \text{Tanh}[(x-x_R-d/2-ct)/w])/2$  and

$F_L(x,t) = (\text{Tanh}[(x-x_L+d/2+ct)/w] - \text{Tanh}[(x-x_L-d/2+ct)/w])/2$ . Here  $x_L$  and  $x_R$  represent the initial center position of the beams,  $d$  is the extension of the beams and  $w$  is the spatial turn-on and off width. Note that we choose this smooth shape in order to eliminate any high-frequency effects associated with a too abrupt spatial turn-on. The temporal duration of the finite beams corresponds to 15 laser periods, out of which 2 periods are associated with the temporal turn-on and -off, based on a  $\sin^2$ -like profile. We also show the two spatially localized incoming fields before the collision.

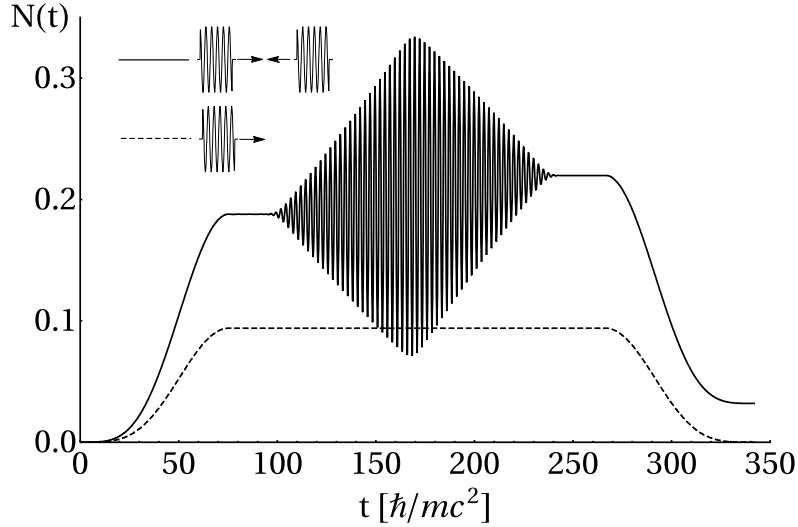


Figure 2 The temporal growth of the numbers of created electron-positron pairs during the interaction of two counter-propagating laser fields with linear polarization. The potential is given by  $\mathbf{A}(\mathbf{r},t) = A_0 [\sin(\omega t - kx) F_R(x,t) + \sin(\omega t + kx) F_L(x,t)] \mathbf{e}_y$ , where the amplitude is such that  $qA_0 = 0.1 mc^2$  and the photon energy  $\hbar\omega = 1.25 mc^2$ . For comparison, the dashed curve shows  $N(t)$  for a single propagating beam,  $\mathbf{A}(\mathbf{r},t) = A_0 \sin(\omega t - kx) F_R(x,t) \mathbf{e}_y$ . We also display the spatial profile of both configurations at the initial time  $t=0$ .

The graph illustrates nicely the above mentioned dual dynamical impact of electromagnetic fields. First, it dresses the vacuum, which leads to the momentary increase of  $N(t)$  to about  $N(t) = 0.1878$ . This dressing manifests itself also in the superimposed rapid oscillations with frequency  $\omega/2$ , whose amplitude ( $N(t) = 0.3339$ ) is maximal around  $t=170 \hbar/(mc^2)$ , when the spatial overlap between the two counter-propagating pulses is largest. As  $N(t)$  was calculated here based on force-free states, we do not associate any physical meaning to the oscillations in  $N(t)$  as they are related to the usual interpretational difficulties with the identifying particles during the interaction [23]. To further illustrate the significance of this dressing, we have indicated by the dashed line for comparison the corresponding yield obtained just from a single propagating pulse, given by  $\mathbf{A}(\mathbf{r},t) =$

$A_0 \sin(\omega t - kx) F_R(x,t) \mathbf{e}_y$ . As expected, here the amount of (reversible) dressing is precisely half of the one for the two pulses.

The true nature of the permanent and irreversible quantum transitions from the Dirac sea to the positive energy states becomes apparent after the two pulses have passed through each other. While the yield  $N(T)$  for the single beam reduces basically to zero ( $5.4 \times 10^{-8}$ ), the final yield  $N(T)$  ( $3.2 \times 10^{-2}$ ) for the two-photon BW process is six orders of magnitude larger.

The sketch of Figure 1 illustrates that both fields  $\mathbf{A}(\mathbf{r},t)$  as well as  $\mathbf{A}(t)$  can trigger for  $\omega = 2.5mc^2/\hbar$  the occurrence of peaks in the energy spectra at  $E = \hbar\omega$  and  $2\hbar\omega$ . In order to compare also the corresponding peak intensities, we have computed the spectra  $\rho(E,T)$  for both configurations. The two spectra after the interaction (displayed in Figure 3 on a logarithmic scale) are entirely different. As expected, the two unphysical peaks at  $1.25 mc^2$  and  $3.75 mc^2$  associated with  $\mathbf{A}(t)$  are absent in the correct data for  $\mathbf{A}(\mathbf{r},t)$ . More interestingly, the intensity of the unphysical peak at  $1.25 mc^2$  [associated with  $\mathbf{A}(t)$ ] is by about eight order of magnitudes larger than predicted by  $\mathbf{A}(\mathbf{r},t)$ , while the physical peak at  $2.5 mc^2$  [for  $\mathbf{A}(\mathbf{r},t)$ ] is about eight orders of magnitude larger than the one obtained for  $\mathbf{A}(t)$ .

We have also monitored the scaling of the peak intensities with the field amplitude  $A_0$ . While the dominant (unphysical) peak at  $E = 1.25\hbar\omega$  grows quadratically in  $A_0$ , the true peak at  $E = \hbar\omega$  grows  $\sim A_0^4$ , which is consistent with two-photon nature of the BW-process. The peak associated with  $4\gamma \rightarrow e^- + e^+$  grows  $\sim A_0^{16}$  and is therefore more difficult to observe experimentally.

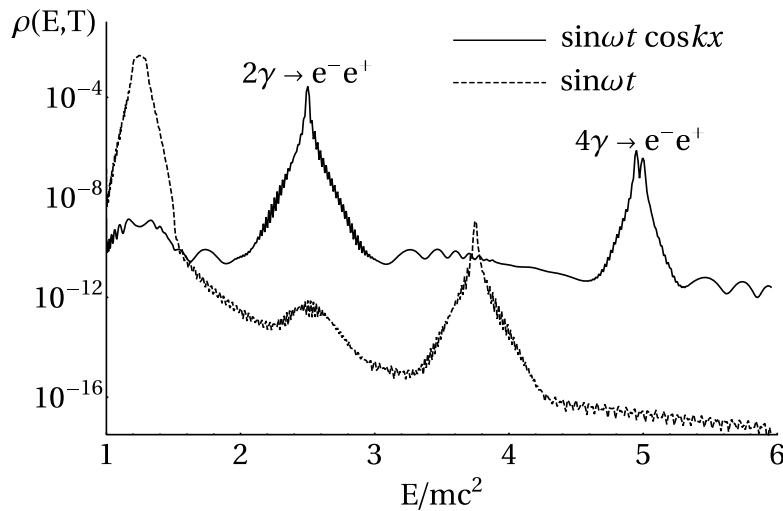


Figure 3 The energy spectrum of the emitted electron-positron pair after the interaction of two

colliding photon beams, modelled  $\mathbf{A}(\mathbf{r},t) = A_0 \sin(\omega t) \cos(kx) \mathbf{e}_y$ , where the amplitude is  $qA_0 = 0.1 \text{ mc}^2$  and the photon energy  $\hbar\omega = 2.5 \text{ mc}^2$ . For comparison, the dashed line displays the corresponding spectrum for the potential  $\mathbf{A}(t) = A_0 \sin(\omega t) \mathbf{e}_y$ , where the crucial spatial dependence has been omitted.

In summary, we have seen that the omission of the crucial spatial dependence of the electromagnetic field leads to entirely different physical results if the laser frequency is as large as required for the BW process. This finding is not so unexpected as the spatial scale characteristic of the spatial inhomogeneity  $\cos(kx)$  is of the order of  $\pi c/\omega$ , which for a typical BW  $\gamma$ -ray photon ( $\hbar\omega = 2.5 \text{ mc}^2$ ) amounts to about  $(\pi/2.5) \lambda_C$ . In other words, the spatial scale is comparable to the electron's Compton wavelength  $\lambda_C (= \hbar/mc)$ . As this minute scale is identical to the scale at which the pair creation process is expected to happen, it is of no surprise that the omission of the spatial inhomogeneity leads to entirely inaccurate predictions. We could therefore expect that for smaller energies  $\hbar\omega$ , the omission of the spatial inhomogeneity might become less serious.

In order to examine this important question more quantitatively, we have computed the pair-creation rate  $\Gamma$  as a function of the photon energy  $\hbar\omega$  and compared it in the left panel of Figure 4 with the corresponding rates associated with the spatially homogeneous field  $\mathbf{A}(t)$ , which we denote by  $\Gamma_H$ . To examine an unambiguous pair creation rate  $\Gamma$ , we have delocalized the two counter-propagating fields by choosing  $F_{R,L}(x,t) = 1$ , such that the observed yield grows linearly as a function of the total duration  $T$  of the interaction,  $N(T) = \Gamma T$ .

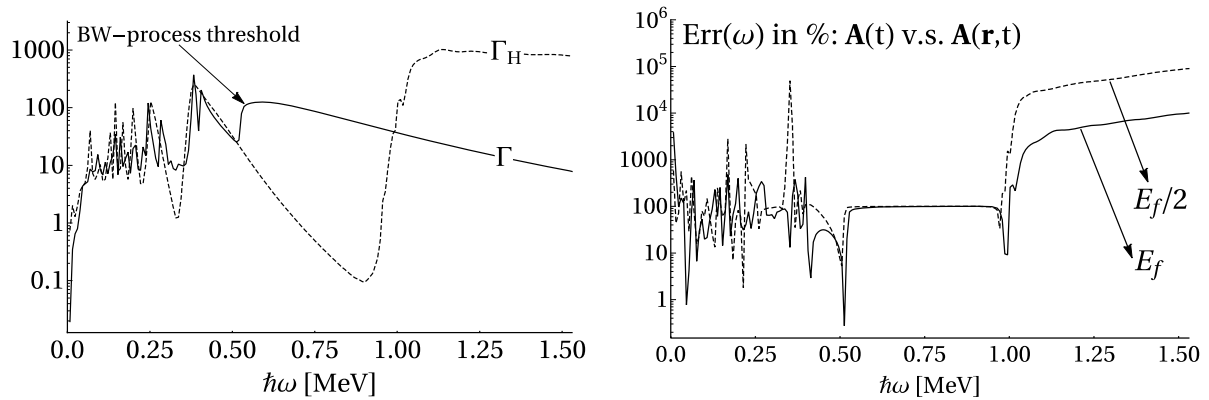


Figure 4

Left panel: The pair-creation rate  $\Gamma$  (graphed in units of  $\text{mc}^2/\hbar$ ) computed from the laser field  $\mathbf{A}(\mathbf{r},t) = A_0 \sin(\omega t) \cos(kx) \mathbf{e}_y$ , and the rate  $\Gamma_H$  computed from the spatially homogeneous field  $\mathbf{A}(t) = A_0 \sin(\omega t) \mathbf{e}_y$ , as a function of the frequency  $\omega$ . The amplitudes  $A_0$  are chosen such that the electric field strength fulfills  $qE_f = 0.1 \text{ m}^2 \text{ c}^3/\hbar$ .

Right panel: The relative error  $\text{Err}(\omega) = |\Gamma - \Gamma_H|/\Gamma$  for the pair-creation rate due to the omission of the spatial inhomogeneity of the external field. The dashed line is the error for half the field strength used in the left panel.

While for smaller laser frequencies ( $\hbar\omega < 0.1\text{MeV}$ ) the two rates have about the same order of magnitude, in the regime ( $0.5\text{MeV} < \hbar\omega < 1\text{MeV}$ ) the rate  $\Gamma$  from the two-pulse configuration is significantly *above* the creation rate  $\Gamma_H$  for the homogeneous field. For even larger frequencies,  $\Gamma_H$  completely overestimates the true rate. This means that here the omission of the magnetic field component of the laser strongly enhances the pair creation. The data therefore suggest that impact of the laser's magnetic field can either increase as well as decrease the total observed particle yield depending on the laser's frequency. This conclusion is in contrast to claims in the literature that the presence of the laser's magnetic field component always reduces the yield [5,22].

In the right panel of Figure 4 we have graphed the relative error of the pair-creation rate, defined as  $\text{Err}(\omega) \equiv |\Gamma - \Gamma_H|/\Gamma$ , as a function of the laser frequency  $\omega$ . We see that the error in the yield for the parameters presented in Figure 3 ( $\hbar\omega = 2.5mc^2 = 1.275\text{MeV}$ ) is about 5654%. Once the frequency decreases below  $\omega = 2mc^2/\hbar$ , the unphysical one-photon transition triggered by the  $\mathbf{A}(t)$  is no longer possible, the error reduces to around 100%.

In conclusion, while prior (and widely cited) works were aware of the "slightly unrealistic character" [6] of the assumption of spatial homogeneity, we believe that the present study provides a quantitative indication of the potential seriousness of such an approximation. It suggests that this simplification does not retain any of the main features of the dynamics in the multiphoton regime. For example, estimates of the pair creation rates that are based on the powerful and frequently used quantum Vlasov equation may become entirely unrealistic, as this particular approach requires the external field to be spatially homogeneous. By investigating the BW-process, we have seen that the tight spatial dependence of the laser significantly affects the electron spectra and it thus has to be taken into account for the design of upcoming strong laser facilities that plan to examine various strong-field QED processes.

A very recent work by Aleksandrov, Plunien and Shabaev [10] has also compared the effect of the dipole and the standing wave approximations. While their numerical approach (based on the quantization of the Furry picture) is different from our approach, its main conclusions about the significant alternations due to the magnetic field are fully consistent with our overall findings. The present work is therefore complementary to Ref. [10] that has a focus on the effects of the

approximations (and also of the carrier-envelope phase and other details of the pulse shape) on the final momentum spectra of the created particles. In this work, we have shown that despite a nontrivial time-dependent dynamics during the interaction, it is possible to describe some aspects of the process by a single rate, and identify specifically those laser-induced transitions that are physical and unphysical. We examined the total pair-creation rate after the interaction for a wide range of frequencies and suggest that depending on the frequency, the omission of the magnetic component can lead to both an enhancement as well as a reduction in the total rate.

This situation is likely more complicated if the laser field does not just act as the sole facilitator of the pair-creation process (as discussed in this work), but it is used to accompany a second (possibly static) supercritical external force field, as required for the dynamically assisted Schwinger process. Here the relevance of the laser's spatial inhomogeneities might require further studies. From some preliminary results, we can see that a spatially homogeneous field  $\mathbf{A}(t)$  will lead to much narrower energy distributions for the created electrons compared to a realistic laser field  $\mathbf{A}(\mathbf{r},t)$ . More systematic studies of this problem will be reported in future work.

We acknowledge helpful discussions with H. Bauke, M. Chen, N. Christensen, A. Di Piazza and C.H. Keitel. QZL and SD would like to thank ILP for the nice hospitality during their visits to Illinois State. This work has been supported by the Alexander von Humboldt Foundation, the NSF, the NSFC (#11529402) and by Research Corporation.

## References

- [1] G. Chériaux, F. Giambruno, A. Fréneaux, F. Leconte, L.P. Ramirez, P. Georges, F. Druon, D.N. Papadopoulos, A. Pellegrina, C. Le Blanc, I. Doyen, L. Legat, J.M. Boudenne, G. Mennerat, P. Audebert, G. Mourou, F. Mathieu and J.P. Chambaret, AIP Conf. Proc. 1462, 78 (2012).
- [2] For a comprehensive review, see A. Di Piazza, C. Müller, K.Z. Hatsagortsyan and C.H. Keitel, Rev. Mod. Phys. 84, 1177 (2012).
- [3] J.S. Schwinger, Phys. Rev. 128, 2425 (1962).
- [4] For early work, see G. Breit and J.A. Wheeler, Phys. Rev. 46, 1087 (1934).
- [5] For a review, see, e.g., V.S. Popov, Physics Uspekhi 47 (9) 855 (2004).
- [6] E. Brezin and C. Itzykson, Phys. Rev. D2, 1191 (1970).
- [7] S.S. Bulanov, N.B. Narozhny, V.D. Mur and V.S. Popov, J. Exp. and Theo. Phys. 102, 9 (2006).
- [8] G.V. Dunne and Q. Wang, Phys. Rev. D 74, 065015 (2006).
- [9] F. Hebenstreit, R. Alkofer, and H. Gies, Phys. Rev. Lett. 107, 180403 (2011).
- [10] I.A. Aleksandrov, G. Plunien and V.M. Shabaev, Phys. Rev. D 96, 076006 (2017).
- [11] S.R. Das, D.A. Galante and R.C. Myers, J. High Energ. Phys. 164, 2016 (2016).
- [12] F. Hebenstreit, R. Alkofer, and H. Gies, Phys. Rev. D 82, 105026 (2010).
- [13] arXiv:1708.08920, “Phase-space analysis of the Schwinger effect in inhomogeneous electromagnetic fields” by C. Kohlfürst.
- [14] I.A. Aleksandrov, G. Plunien, and V.M. Shabaev, Phys. Rev. D 94, 065024 (2016).
- [15] O.J. Pike, F. Mackenroth, E.G. Hill and S.J. Rose, Nature Phot. 8, 434 (2014).
- [16] A. Thomas, Nature Phot. 8, 429 (2014).
- [17] X. Ribeyre, E. d'Humières, O. Jansen, S. Jequier, V.T. Tikhonchuk and M. Lobet, Phys. Rev. E 93, 013201 (2016).
- [18] C. Bamber, S.J. Boege, T. Koffas, T. Kotseroglou, A.C. Melissinos, D.D. Meyerhofer, D. A. Reis, W. Ragg, C. Bula, K.T. McDonald, E.J. Prebys, D.L. Burke, R.C. Field, G. Horton-Smith, J.E. Spencer, D. Walz, S.C. Berridge, W.M. Bugg, K. Shmakov and A.W. Weidemann, Phys. Rev. D 60, 092004 (1999).
- [19] C. Gahn, G. D. Tsakiris, G. Pretzler, K.J. Witte, C. Delfin, C.G. Wahlstrom and D. Habs, Appl. Phys. Lett. 77, 2662 (2000).
- [20] H. Chen, S.C. Wilks, J.D. Bonlie, E.P. Liang, J. Myatt, D.F. Price, D.D. Meyerhofer and P.

- Beiersdorfer, Phys. Rev. Lett. 102, 105001 (2009).
- [21] P. Krekora, Q. Su and R. Grobe, Phys. Rev. Lett. 92, 040406 (2004).
- [22] M. Ruf, G.R. Mocken, C. Müller, K.Z. Hatsagortsyan and C.H. Keitel, Phys. Rev. Lett. 102, 080402 (2009).
- [23] P. Krekora, Q. Su and R. Grobe, Phys. Rev. A 73, 022114 (2006).